COMMUNICATION

Electrochemically Induced Iodine Migration in Mixed Halide Perovskites: Suppression through Chloride Insertion

Received 00th January 20xx,
Accepted 00th January 20xx

DOI: 10.1039/x0xx00000x

Junsang Cho[1], Jeffrey T. DuBose[1,2], Preethi S. Mathew[1,2], and Prashant V. Kamat[1,2,3*]

The role of chloride in improving the stability of mixed halide perovskites ($MAPbCl_xBr_{0.5(1-x)}I_{0.5(1-x)})_3$ is probed using spectroelectrochemistry. The injection of holes into mixed halide perovskite films through applied anodic bias results in the selective migration of iodine with ultimate expulsion into the electrolyte. Increasing the Cl content (*x* = 0 to 0.1) in the mixed halide perovskite suppresses the iodine mobility and thus decreases the rate of its expulsion into the solution. Implication of iodine mobility induced by hole accumulation and its impact on overall stability is discussed.

The composition of cation and anion in metal halide perovskites plays an important role in determining overall integrity, film stability and photovoltaic performance of solar cells.[1-4] Of particular interest is halide ion migration in perovskite films which has been a key discussion topic for improving the performance and stability of photovoltaic and display devices.[4-11] Mixed halide perovskites offer a convenient way to probe the movement of individual halide ions by tracking the spectral characteristics of different halide rich regions.[12-19] For example, when methyl ammonium lead bromide/iodide ($MAPb(Br_xI_{1-x})_3$) films are subjected to photoirradiation, they undergo phase segregation. The formation of iodide rich and bromide rich regions can be monitored through absorption and emission changes during photoirradiation. The excitation energy needs to overcome entropy of mixing of two halides to induce phase segregation.[20] An extreme situation is the expulsion of one of the halide species from the mixed halide films. Indeed, when $MAPbBr_{1.5}I_{1.5}$ films were in contact with a solvent, iodine species can be expelled into the solution through the injection of holes.[21] Both electrochemical and photochemical injection of holes which is responsible for iodide migration can introduce such a selective expulsion of iodide.[22-24]

The introduction of an additional *A-site* cation (e.g. cesium (Cs), formamidinium(FA)) has been shown to improve the stability of perovskite solar cells.[1, 2] In our previous study we have shown that replacing MA with Cs can suppress both photoinduced segregation and expulsion of iodide in $MAPbBr_{1.5}I_{1.5}$ films.[21] Similarly, introduction of Cl in the perovskite film also improves the solar cell stability.[25-30] In order to further assess the role of chloride on the mobility of other halide ions (viz., Br and I) we have now conducted electrochemical experiments by selectively injecting holes into mixed halide films. Unlike photoirradiation experiments, in which both charge carriers are produced, electrochemical modulation allows selective injection of electrons or holes.

Mixed halide perovskite films were cast on FTO (fluorine doped tin oxide) using the procedure described earlier.[20, 21, 23, 24] Details are also provided in the Electronic Supplementary Information (ESI). The stability of the perovskite film in dichloromethane (DCM) containing 0.1 M and 0.01 M tetrabutylammonium hexafluorophosphate (Bu_4NPF_6) were separately tested by recording absorption spectra (See **Fig. S1** in the ESI). No changes in the absorption could be seen when the concentration was maintained at 0.01 M Bu_4NPF_6 during the period of 30 minutes. These control experiments attested to the stability of these perovskite films for conducting electrochemical experiments. The mixed halide perovskite-coated FTO electrode (working electrode), Pt counter electrode, and Ag/AgCl reference electrode were introduced in a spectroelectrochemical cell. The absorption spectra were recorded using Cary 50 Bio spectrophotometer (Varian) at different applied potentials using a Gamry potentiostat.

In our previous study we laid out the necessary conditions to carry out electrochemical experiments with perovskite films.[23, 31] Upon application of anodic bias one can selectively inject holes into perovskite film and observe transformations through absorption

[1]*Radiation Laboratory,* [2]*Department of Chemistry and Biochemistry, and*
[3]*Department of Chemical and Biomolecular Engineering, University of Notre Dame, Notre Dame, Indiana 46556, United States*
[*]*Corresponding Author: pkamat@nd.edu*
Electronic Supplementary Information (ESI) available: [details of experimental section, steady-state absorption spectra, difference absorption spectra, SEM images, and kinetic fitting parameters]. See DOI: 10.1039/x0xx00000x

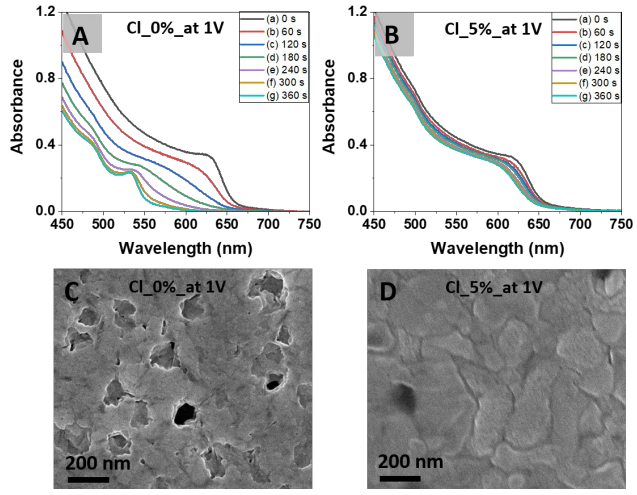

Fig. 1 (A,B) Absorbance changes recorded for FTO/MAPb($Cl_xBr_{0.5(1-x)}I_{0.5(1-x)}$)$_3$ films with (A) 0% Cl and (B) 5% Cl during anodic bias of 1.0 V versus Ag/AgCl in 0.01 M Bu_4NPF_6/DCM electrolyte for 0-360 s (a-g). (C,D) Corresponding top-down SEM images of the films with (C) 0%_Cl and (D) 5%_Cl after potentiostatic treatment (1.0 V vs Ag/AgCl) for 360 s (corresponding to spectrum g of A,C).

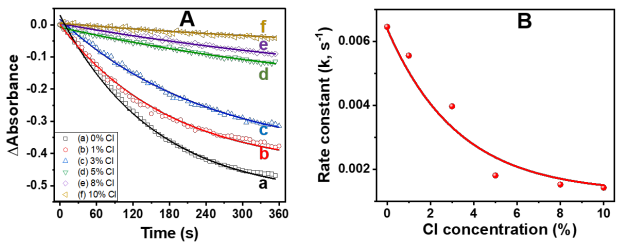

Fig. 2 (A) Change in absorbance at 500 nm and first order kinetic fit (solid line) for the FTO/MAPb($Cl_xBr_{0.5(1-x)}I_{0.5(1-x)}$)$_3$ films with different Cl concentration from 0-10% (a-f) while maintaining a constant anodic bias of 1.0 V vs. Ag/AgCl in 0.01 M Bu_4NPF_6/DCM electrolyte. (B) Dependence of rate constant (k, s^{-1}) of iodide expulsion extracted from the kinetic trace fittings of panel A using monoexponential fits on chloride concentration in the mixed halide film.

spectroscopy. **Figs. 1A and B** show changes in the absorption spectra of $MAPbBr_{1.5}I_{1.5}$ films with and without the presence of chloride after subjecting the film to 1.0 V *vs.* Ag/AgCl. In the absence of Cl we observe a continuous shift of absorption to the blue. The change in absorption is similar to what we observe when iodine from mixed halide film is expelled into the solution.[21, 23] After about 300 seconds the absorption represents the absorption characteristics of $MAPbBr_3$ with an excitonic band at 530 nm. No additional change in the absorption is seen when we continue to apply bias for a longer time. This suggests that only iodide in the mixed halide perovskite film is mobile and gets expelled into the solution. (The dependence of excitonic peak on Cl concentration in the mixed halide is presented in **Fig. S2** (ESI)) The mechanistic details of iodide expulsion can be found elsewhere.[21, 23]

When the same experiment was conducted with a mixed halide film containing 5% Cl, the shift in absorption is much smaller indicating a slower rate of iodide expulsion. **Figs. 1C and D** show the scanning electron microscopy (SEM) images recorded after application of 1.0 V vs. Ag/AgCl for 360 s. The SEM images of these films prior to application of anodic bias are presented in **Fig. S3** (ESI). The morphology of the film shows holes within the film as they were subjected to anodic bias. The deformation of the surface with holes is more evident for $MAPbBr_{1.5}I_{1.5}$ films (0% Cl) than the one containing 5% Cl. The degree of the surface transformation is in line with the absorption changes in Figs. 1A and B. The expulsion of iodine and restructuring of the film during the anodic bias is described in expression 1.

$$2MAPbBr_{1.5}I_{1.5} + h^+ \rightarrow (MAPbBr_3)PbI_2 + MA^+ + \frac{1}{2}I_2 \qquad (1)$$

The experiments described in Fig. 1 were repeated using different concentrations of Cl in the mixed halide (MAPb($Cl_xBr_{0.5(1-x)}I_{0.5(1-x)}$)$_3$) film (see **Figs. S4 and S5** (ESI) for changes recorded in the absorption spectra of different films). We monitored the loss of absorption at 500 nm to estimate the rate of expulsion of I (**Fig. 2A**). The rate of decrease of I expulsion is influenced strongly by the presence of Cl in the film. With increasing concentration of Cl (x = 0 to 0.1 or 0-10% of halide content) we see a steady decrease in the rate constant of iodide expulsion. The plot of rate constant of I expulsion on the Cl content shows that only a small amount (x = 0.05 or 5% of halide content) of Cl in mixed halide perovskite (MAPb($Cl_xBr_{0.5(1-x)}I_{0.5(1-x)}$)$_3$) is sufficient to slow down the iodide expulsion by a factor of >3 (**Fig. 2B**). Similar influence of Cl on the mobility of iodide was also noted in our earlier studies related to photoinduced segregation of halides in mixed halide films.[32,33] The major difference of the present study is the exclusive influence of selective hole injection through applied electrochemical bias. This indirectly supports the argument that holes trapped at the iodide sites makes it labile and move towards the grain boundaries. It is interesting to note that perovskite solar cell stability studies point out the importance of chloride treatment as a key step to improve the stability.[4, 25, 27, 28, 30]

In order to further probe the influence of Cl on the band energies of mixed halide perovskites, we evaluated the voltammetry performance of mixed halide perovskite films containing different amounts of Cl. **Fig. 3A** shows the linear sweep voltammograms acquired for the FTO/MAPb($Cl_xBr_{0.5(1-x)}I_{0.5(1-x)}$)$_3$ films containing different Cl concentration (from 0-10%) in 0.01 M Bu_4NPF_6/DCM medium. The linear voltammograms of mixed halide films show two distinct peaks. As we sweep the electrochemical bias in the anodic region, holes get trapped in the mixed halide film initially at sites near the valence band. This trapping of holes is seen as a pre-peak around 0.85 V vs. Ag/AgCl (identified as 1st peak in **Figs. 3A** and **S6** in the ESI). As we sweep the bias to positive potentials (anodic scan), we see injection of holes into the valence band of mixed halide films (identified as 2nd peak in **Fig. 3A**). This second peak which exhibits large anodic current has been used to identify valence band

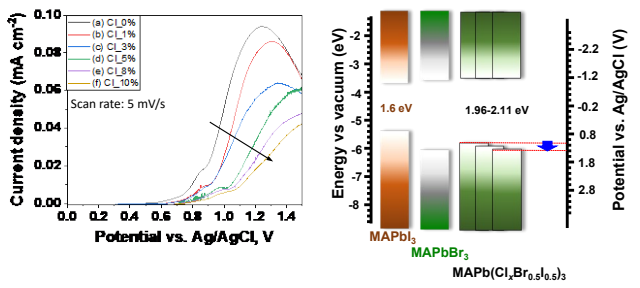

Fig. 3 (A) Linear sweep voltammograms acquired for the FTO/MAPb($Cl_xBr_{0.5(1-x)}I_{0.5(1-x)}$)$_3$ films with different Cl concentration from 0-10% (a-f) with a scan rate of 5 mV/s in the voltage range of 0-1.5 V vs. Ag/AgCl in 0.01 M Bu_4NPF_6/DCM electrolyte. The first peak corresponds to electrochemical hole trapping in the perovskite film. (B) Band diagram of $MAPbBr_3$, $MAPbI_3$, and mixed MAPb($Cl_xBr_{0.5(1-x)}I_{0.5(1-x)}$)$_3$ relative to vacuum energy (left) and Ag/AgCl (right).

positions. Detailed identification of voltammetry peaks corresponding to the hole injection is discussed in our previous study.[23]

It is interesting to note that inclusion of even a small amount of Cl leads to the shift in the anodic peak positions to more positive potentials. For example, the peak position corresponding to hole trapping (1st peak) shifts from 0.85 V to 1.02 V vs. Ag/AgCl as the Cl concentration was increased to 10%. Similarly, the 2nd peak shifts from 1.25 V to 1.4 V vs. Ag/AgCl. The shift in these peaks is consistent with the shift in the increase in the valence band position (~0.15 V) of mixed halide perovskites. Note that inclusion of Cl (from 0 to 10%) increases the bandgap from 1.96 eV to 2.11 eV (Fig. S2 in the ESI) and most of this increase arises from the shift in valence band position which is dictated by the halide ions in the perovskite lattice. The illustration of the energy band diagram depicting conduction and valence band positions is shown in **Fig. 3B**. These electrochemical experiments further point out that both hole trapping and hole injection becomes energetically more difficult as we increase the Cl content in the film.

Spectroelectrochemical experiments were conducted to probe the absorption change as a function of applied potential. **Fig. 4A** shows the absorption monitored at 500 nm along with the current versus applied potential of the FTO/$MAPbBr_{1.5}I_{1.5}$ electrode in DCM containing 0.01 M Bu_4NPF_6. In the non-Faradaic current region (<0.85 V vs. Ag/AgCl) the absorption remains steady, indicating no changes in the film composition. At potentials greater than 0.85 V we first see a slow decrease in absorption until ~1.0 V and then a rapid decrease in the absorption. More than 60% absorption decrease is seen at 1.4 V. These results confirm that the hole injection into the mixed halide film is the primary event leading to the changes in the absorption. As evident from the absorption spectrum recorded in Fig. 1A, these changes reflect expulsion of iodide leaving behind a $MAPbBr_3$/PbI_2 composition.[21, 23] We repeated similar spectroelectrochemical experiment with different concentrations of Cl in the mixed halide

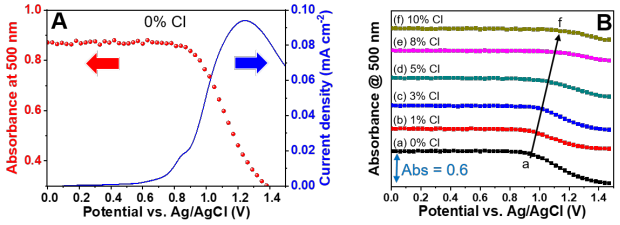

Fig. 4. (A) Linear sweep voltammogram (right axis, blue trace) and corresponding absorption change at 500 nm (left axis, red trace) for the mixed halide film ($MAPbBr_{1.5}I_{1.5}$) deposited on FTO in 0.01 M Bu_4NPF_6/DCM electrolyte. (B) Absorption changes monitored at 500 nm for films with different Cl concentration from 0-10% (a-f) under applied anodic bias.

perovskite film (**Fig. S7** in the ESI). The absorption changes at 500 nm extracted from these spectra are presented in **Fig. 4B**. As expected, the onset of the absorption change shifts to more positive potentials and the net change in the absorbance becomes smaller with increasing concentration of Cl (0-10%) in the mixed halide film. These experiments further confirm the stabilizing role of Cl by suppressing the mobility and hence the expulsion of iodide in the mixed halide perovskite film.

When perovskite films are subjected to photoirradiation, *e.g.*, during the operation of a solar cell, both charge carriers (electron and holes) are produced. Similarly, in light emitting diodes, electrons and holes are injected into the perovskite film so that these charge carriers recombine radiatively to produce light emission. Quick transport of both charge carriers for photocurrent generation or light emission is important as they need to be transported through electron transport layer (ETL) and hole transport layer (HTL). In order to maintain good stability, it is important to maintain similar rates of charge transport across ETL and HTL. Any mismatch of transport rate can lead to accumulation of one of the charge carriers. Such an accumulation of charge carriers in turn can build up capacitance or induce chemical transformations.[24] By employing selective injection of holes into mixed halide perovskite through externally applied electrochemical bias, we were able to show the effect of excess holes trapped into iodide sites and its mobility in mixed perovskite films. As an example of the extreme case, we could expel iodine from the mixed halide perovskite film as we inject holes into the film. Interestingly, the presence of Cl in mixed halide perovskite film, even at very low concentration (<5%) is sufficient to suppress the iodide mobility and its expulsion. The observed effect of chloride in stabilizing the perovskite structure is in agreement with the decreased segregation of Br and I in mixed halide films and improving the photostability of solar cells.

Acknowledgement

We (J.T.D. and P.V.K.) acknowledge support by the Division of Chemical Sciences, Geosciences, and Biosciences, Office of Basic Energy Sciences of the U.S. Department of Energy (award DE-FC02-04ER15533) for conducting spectroelectrochemical measurements

and discussions. P.S.M. acknowledges the Division of Materials Sciences and Engineering Office of Basic Energy Sciences of the U.S. Department of Energy through Award DE-SC0014334 for assisting in iodide expulsion experiments and discussions. This is contribution number NDRL No. 5296 from the Notre Dame Radiation Laboratory.

Conflicts of interest

There are no conflicts to declare.

References

1 D. P. McMeekin, G. Sadoughi, W. Rehman, G. E. Eperon, M. Saliba, M. T. Hörantner, A. Haghighirad, N. Sakai, L. Korte, B. Rech, M. B. Johnston, L. M. Herz and H. J. Snaith, *Science*, 2016, **351**, 151-155.
2 M. Saliba, T. Matsui, J.-Y. Seo, K. Domanski, J.-P. Correa-Baena, M. K. Nazeeruddin, S. M. Zakeeruddin, W. Tress, A. Abate, A. Hagfeldt and M. Grätzel, *Energy Environ. Sci.*, 2016, **9**, 1989-1997.
3 K. Poorkazem and T. L. Kelly, *ACS Appl. Energy Mater.*, 2018, **1**, 181-190.
4 J. Xu, C. C. Boyd, Z. J. Yu, A. F. Palmstrom, D. J. Witter, B. W. Larson, R. M. France, J. Werner, S. P. Harvey, E. J. Wolf, W. Weigand, S. Manzoor, M. F. A. M. van Hest, J. J. Berry, J. M. Luther, Z. C. Holman and M. D. McGehee, *Science*, 2020, **367**, 1097-1104.
5 J. M. Frost and A. Walsh, *Acc. Chem. Res.*, 2016, **49**, 528-535.
6 C. Li, S. Tscheuschner, F. Paulus, P. E. Hopkinson, J. Kiessling, A. Kohler, Y. Vaynzof and S. Huettner, *Adv. Mater.*, 2016, **28**, 2446-2454.
7 A. H. Slavney, R. W. Smaha, I. C. Smith, A. Jaffe, D. Umeyama and H. I. Karunadasa, *Inorg. Chem.*, 2017, **56**, 46-55.
8 S. T. Birkhold, J. T. Precht, H. Liu, R. Giridharagopal, G. E. Eperon, L. Schmidt-Mende, X. Li and D. S. Ginger, *ACS Energy Lett.*, 2018, **3**, 1279-1286.
9 R. A. Belisle, K. A. Bush, L. Bertoluzzi, A. Gold-Parker, M. F. Toney and M. D. McGehee, *ACS Energy Lett.*, 2018, **3**, 2694-2700.
10 Z. Huang, A. H. Proppe, H. Tan, M. I. Saidaminov, F. Tan, A. Mei, C.-S. Tan, M. Wei, Y. Hou, H. Han, S. O. Kelley and E. H. Sargent, *ACS Energy Lett.*, 2019, DOI: 10.1021/acsenergylett.9b00892, 1521-1527.
11 M. J. Hong, R. Y. Johnson and J. G. Labram, *J. Phys. Chem. Lett.*, 2020, **11**, 4976-4983.
12 E. T. Hoke, D. J. Slotcavage, E. R. Dohner, A. R. Bowring, H. I. Karunadasa and M. D. McGehee, *Chem. Sci.*, 2015, **6**, 613-617.
13 S. J. Yoon, S. Draguta, J. S. Manser, O. Sharia, W. F. Schneider, M. Kuno and P. V. Kamat, *ACS Energy Lett.*, 2016, **1**, 290-296.
14 E. L. Unger, L. Kegelmann, K. Suchan, D. Sörell, L. Korte and S. Albrecht, *J. Mater. Chem. A*, 2017, **5**, 11401-11409.
15 M. C. Brennan, S. Draguta, P. V. Kamat and M. Kuno, *ACS Energy Lett.*, 2018, **3**, 204-213.
16 A. J. Knight, A. D. Wright, J. B. Patel, D. P. McMeekin, H. J. Snaith, M. B. Johnston and L. M. Herz, *ACS Energy Lett.*, 2019, **4**, 75-84.
17 A. F. Gualdrón-Reyes, S. J. Yoon and I. Mora-Seró, *Curr. Opin. Electrochem.*, 2018, **11**, 84-90.
18 A. F. Gualdrón-Reyes, S. J. Yoon, E. M. Barea, S. Agouram, V. Muñoz-Sanjosé, Á. M. Meléndez, M. E. Niño-Gómez and I. Mora-Seró, *ACS Energy Lett.*, 2019, **4**, 54-62.
19 J. R. Vicente and J. Chen, *J. Phys. Chem. Lett.*, 2020, **11**, 1802-1807.
20 T. Elmelund, B. Seger, M. Kuno and P. V. Kamat, *ACS Energy Lett.*, 2020, **5**, 56-63.
21 P. S. Mathew, G. F. Samu, C. Janáky and P. V. Kamat, *ACS Energy Lett.*, 2020, **5**, 1872-1880.
22 G. Y. Kim, A. Senocrate, T.-Y. Yang, G. Gregori, M. Grätzel and J. Maier, *Nat. Mater.*, 2018, **17**, 445-449.
23 G. F. Samu, Á. Balog, F. De Angelis, D. Meggiolaro, P. V. Kamat and C. Janáky, *J. Am. Chem. Soc.*, 2019, **141**, 10812-10820.
24 J. T. DuBose and P. V. Kamat, *J. Am. Chem. Soc.*, 2020, **142**, 5362-5370.
25 E. Edri, S. Kirmayer, M. Kulbak, G. Hodes and D. Cahen, *J. Phys. Chem. Lett.*, 2014, **5**, 429-433.
26 S. Colella, E. Mosconi, P. Fedeli, A. Listorti, F. Gazza, F. Orlandi, P. Ferro, T. Besagni, A. Rizzo, G. Calestani, G. Gigli, F. De Angelis and R. Mosca, *Chem. Mater.*, 2013, **25**, 4613-4618.
27 S. T. Williams, F. Zuo, C.-C. Chueh, C.-Y. Liao, P.-W. Liang and A. K. Y. Jen, *ACS Nano*, 2014, **8**, 10640-10654.
28 S. Dastidar, D. A. Egger, L. Z. Tan, S. B. Cromer, A. D. Dillon, S. Liu, L. Kronik, A. M. Rappe and A. T. Fafarman, *Nano Lett.*, 2016, **16**, 3563-3570.
29 H. Zhang, Y. Lv, J. Wang, H. Ma, Z. Sun and W. Huang, *ACS Appl. Mater. Interfaces*, 2019, **11**, 6022-6030.
30 D. Ma, P. Todorović, S. Meshkat, M. I. Saidaminov, Y.-K. Wang, B. Chen, P. Li, B. Scheffel, R. Quintero-Bermudez, J. Z. Fan, Y. Dong, B. Sun, C. Xu, C. Zhou, Y. Hou, X. Li, Y. Kang, O. Voznyy, Z.-H. Lu, D. Ban and E. H. Sargent, *J. Am. Chem. Soc.*, 2020, **142**, 5126-5134.
31 G. F. Samu, R. A. Scheidt, P. V. Kamat and C. Janáky, *Chem. Mater.*, 2018, **30**, 561-569.
32 J. Cho and P. V. Kamat, *Chem. Mater.*, 2020, **32**, 6206–6212.
33 J. Cho and P. V. Kamat, *Advanced Optical Materials* **2020,** 8, Art. no. 2001440.

